Bistatic Radar Observations of 2011 UW158

© **A. Ipatov**[1], **Yu. Bondarenko**[1], **Yu. Medvedev**[1], **N. Mishina**[1], **D. Marshalov**[1], **L. A. M. Benner**[2]

[1]Institute of Applied Astronomy of the Russian Academy of Sciences, Saint Petersburg, Russia
[2]Jet Propulsion Laboratory, California Institute of Technology, USA

We report the results of our intercontinental bistatic radar observations of the near-Earth Asteroid 2011 UW158 during its close approach to the Earth in July 2015. A high power continuous wave signal at a fixed 8.4 GHz frequency was transmitted to the asteroid from the 70 m antenna of the Goldstone Observatory (DSS-14) and then the echo was reflected back from the target and received by the 32 m radio telescopes of the "Quasar" VLBI network in the Zelenchukskaya and Badary observatories. An analysis of the echo power spectra allowed us to estimate the size and spin period, which agrees with the photometric observations as well as to obtain some information about the asteroid's shape and its near-surface roughness. Also, we report 18 Doppler estimates and suggest our computed images of the 2011 UW158's heliocentric orbit.

Keywords: Near-Earth objects, Asteroids, Radar observations, Orbit determination.

1 Introduction

Today, radar astronomy is one of the most effective techniques to determine the physical properties of near-Earth asteroids (NEAs). The size, shape, spin period, surface properties, as well as more accurate orbital elements of NEAs can be obtained using radar observations. In this paper, we present the bistatic radar observations and physical properties of the near-Earth asteroid 2011 UW158. This asteroid was discovered on October 25th, 2011 by Pan-STARRS 1 in Maui, USA. Its spin period was reported to be 0.61 h (Gary, 2016) with an absolute magnitude of 20 mag, suggesting a diameter of roughly 450 m. This object made a close approach to the Earth at a distance

of 0.0164 AU on July 19th, 2015. Such absolute magnitude and approach distance yields a sufficient signal-to-noise ratio (SNR) at the 32 m radio telescopes of the "Quasar" VLBI network (Ipatov, 2014).

The intercontinental radar observations of 2011 UW158 were scheduled by the Institute of Applied Astronomy in cooperation with the Goldstone Observatory using 70 m antenna (DSS-14) to transmit signals and 32 m radio telescopes (RT-32) of the "Quasar" VLBI network in the Zelenchukskaya and Badary observatories to receive the echoes. Such type of radar observations is called 'bistatic', where the transmitter and receiver are located on different antennas (Zaitsev et al. 1997). Bistatic observations have a number of advantages. First of all, there is no need to switch the antenna between signal transmission and echo receiving. It is also possible to receive the echoes using several antennas in the interferometric mode. The bistatic observations allow us to continuously observe rapidly rotating celestial bodies, and, in case of the interferometric mode, to estimate the direction of rotation and to obtain more accurate positional observations.

2 Observations and data processing

We observed 2011 UW158 from 20:25 to 21:00 UT on July 18th. During this time the DSS-14 radar was transmitting a circularly polarized continuous wave (CW) signal at 8560 MHz (3.5 cm). The RT-32 radio telescopes in the Zelenchukskaya and Badary observatories received the reflected signal. We used two separate channels to receive the echoes in the same (SC) and opposite (OC) circular polarizations as that of the transmitted wave. The received echo was sampled by the R1002M Data Acquisition System and recorded by the Mark 5B (Grenkov et al. 2010). The R1002M system converted and sampled the received signal in the 0.5 MHz bandwidth. Having applied the fast Fourier transform to the echo time series, we obtained CW echo power spectra at one-second intervals with a frequency resolution of 1 Hz. Henceforth, we combined these spectra to choose the time intervals and their SNR taking into account the Doppler frequency as a function of time.

3 Analysis of spectra

Fig. 1 and Fig. 2 show weighted sums of all CW spectra at Zelenchukskaya and Badary. These spectra give the SNR of about 215 for the OC polarization. Echo power is plotted in standard deviations versus Doppler frequency relative to the estimated frequency of echoes from the asteroid's center of mass. Solid and dashed lines denote echo power in the OC and SC polarizations. Circular polarization of the signal is reversed after its reflection from the plane surface. The maximal power of the reflected signal is expected in the OC polarization, though some of the signal is received with the same po-

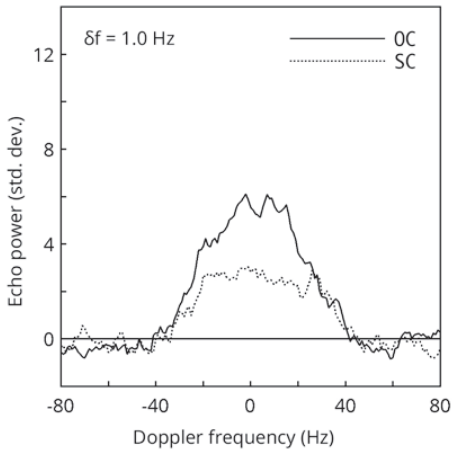

Fig. 1. Opposite- and same-circularization continuous wave echo power spectra obtained at the Zelenchukskaya observatory

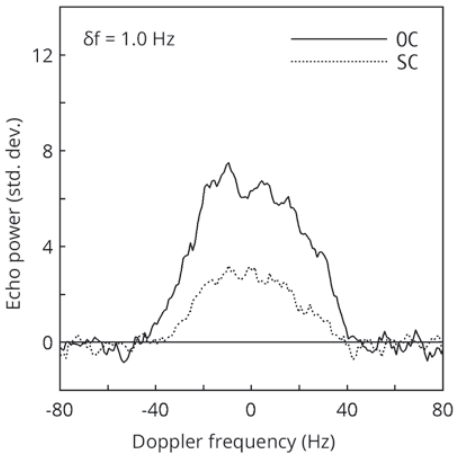

Fig. 2. Opposite- and same-circularization continuous wave echo power spectra obtained at the Badary observatory

larization due to secondary reflections. The ratio of SC to OC is a measure of near surface wavelength-scale roughness (Benner et al., 2008). This circular polarization ratio is often denoted by μC. We obtain circular polarization ratios $\mu C = 0.56 \pm 0.06$ and $\mu C = 0.37 \pm 0.04$ for the Zelenchukskaya and Badary observatories. This ratios are close to the known values $\mu C = 0.34 \pm 0.25$ for the majority of NEAs, which implies that the near-surface roughness is an average at centimeter-to-decimeter spatial scales.

4 Physical model

We have obtained two series of 9 CW echo power spectra for each observatory spanning 30◦ of rotation phase with the 200 sec integration time per spectrum with SNRs of about 70. These spectrums in both OC and SC polarization are shown in Fig. 5 and Fig. 6 for the Badary (Series 1) and Zelenchukskaya (Series 2) observatories respectively. Series 1 and 2 spectra are plotted on identical linear scales of echo power versus the Doppler frequency. The power spectrum bandwidth as function of UTC for both series is given in Fig. 3. Values of the bandwidth for Series 1 and 2 are indicated with black and white dots. The solid curve shows the best-fit average function to the bandwidth values and indicates a spin period of 36 ± 3 min, which is close to the reported light curve period (Gary, 2016). Taking the geometric relation between the echo power spectrum and the shape of the rotating asteroid (Ostro et al. 1990) into account, we estimate a hull of 2011 UW158's polar silhouette. Knowing the obtained spin period and assuming that the spectrum bandwidth is a continuous vector function of the rotation phase we can use least squares to fit the 3-harmonic Fourier series to the data vector. The result is a two-dimensional convex hull which is a projection of the asteroid onto its equatorial plane. In order to convert Hz into meters we can assume that the asteroid-centered declination of the radar is equal to zero. We have considered solutions for each of the observatories separately and our joint solution for both observatories is shown in Fig. 4. The solid profile represents the joint solution and the dotted profiles correspond to the observatories individually. The Earth is toward the bottom of the Fig. 4 and the hull rotates clockwise about its center of mass. The figure shows that the body has an elongated shape with dimensions varying from 350 to 520 meters, which is consistent with the radar observations of the Arecibo Observatory, Green Bank and Goldstone (Naidu et al. 2015).

Taking the geometric relation between echo power spectrum and the shape of rotating asteroid (Ostro et al. 1990) into account, we estimate hull of 2011 UW158 polar silhouette. Knowing the obtained spin period and assuming that the spectrum bandwidth is a continuous vector function of rotation phase we use least squares to fit an 3-harmonic Fourier series to the data vector. The result is a two-dimensional convex hull which is a projection of the asteroid onto its equatorial plane. To convert Hz to meters we assumed that the asteroid-centered declination of the radar is equal to zero. We have considered solutions for each of the observatories separately and a joint solution for both observatories shown in Fig. 4. The solid profile represents the joint solution and the dotted profiles correspond to the observatories individually. The Earth is toward the bottom of the Fig. 4 and the hull rotates clockwise about its center of mass. The figure shows that the body has an

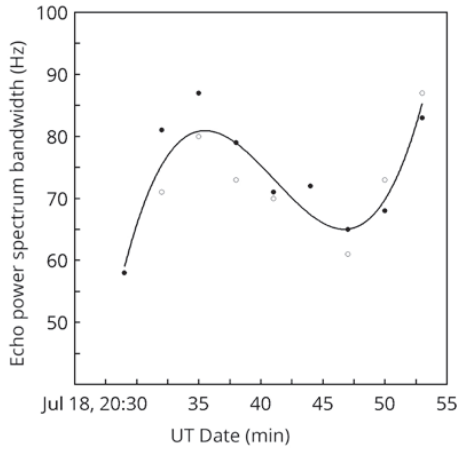

Fig. 3. Echo power spectrum bandwidth as function of UTC

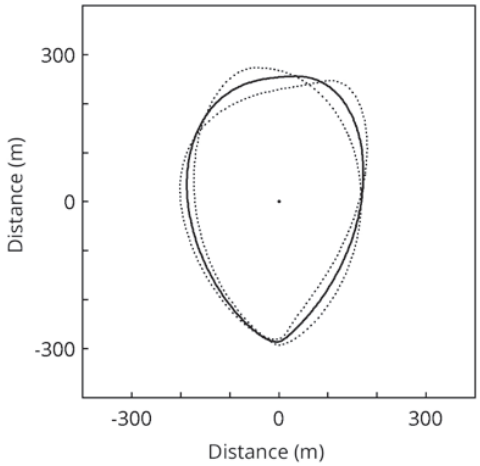

Fig. 4. The convex hull of 2011 UW158's polar silhouette

elongated shape with dimensions varies from 350 to 520 meters, which is consistent with the radar observations of the Arecibo Observatory, Green Bank and Goldstone (Naidu et al. 2015).

Above each spectrum on Fig. 5 and Fig. 6 is a replica of the 2011 UW158 hull (the dotted profiles in Fig. 4), drawn at the same linear scale as the Doppler axis and at the corresponding rotation phase. The UTC midpoint of each rotation phase is indicated. It represents the relation between the orientation of the hull to the line of sight and the shape of the spectrum over time.

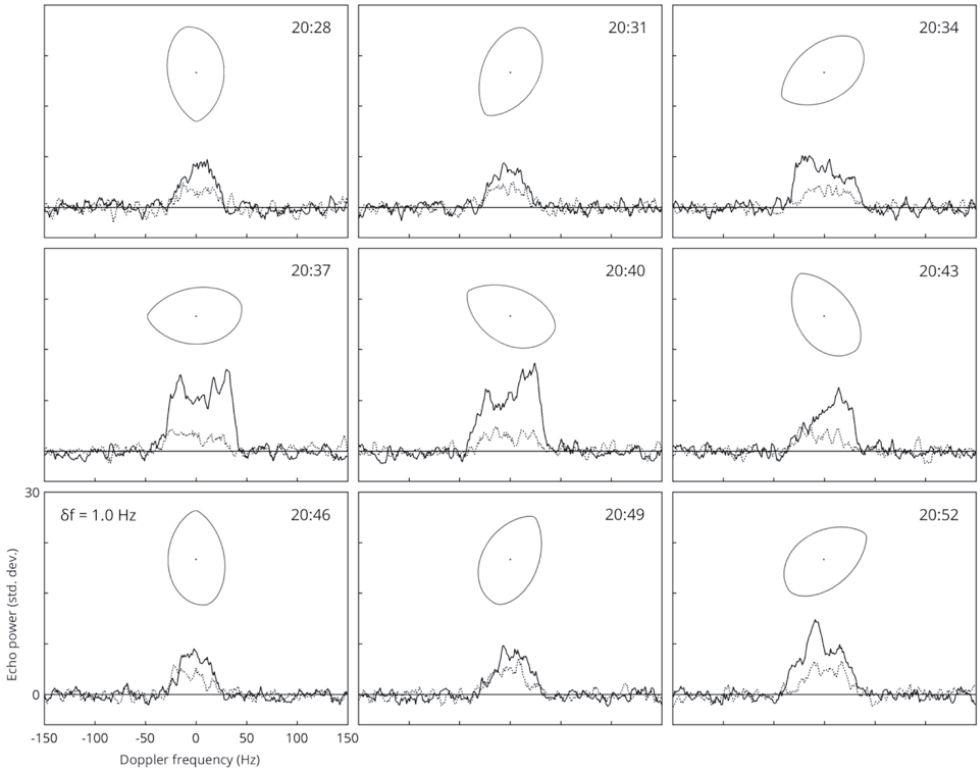

Fig. 5. 2011 UW158's echo spectra and the hull at 9 rotation phases obtained at the Badary observatory

5 Astrometry and orbit

We have obtained 18 Doppler frequency estimates for each spectrum of Series 1 and Series 2, which is shown in Table 2. The orbit of 2011 UW158 was calculated after 921 optical observations, 8 range and 18 our Doppler observations in order to determine uncertainties of Doppler measurements (Bondarenko et al. 2014). The optical observations span October 2011 to November 2015. Table 1 lists the best fit orbital elements and their uncertainties. The Minimum Orbit Intersection Distance with respect to the Earth is 0.0026126 AU, making 2011 UW158 a potentially hazardous asteroid.

The $O - C$ values for the Doppler frequency observations are listed in Table 2. The RMS error is equal to 4 Hz, which is close to the expected value, based on the accuracy of the described calculations.

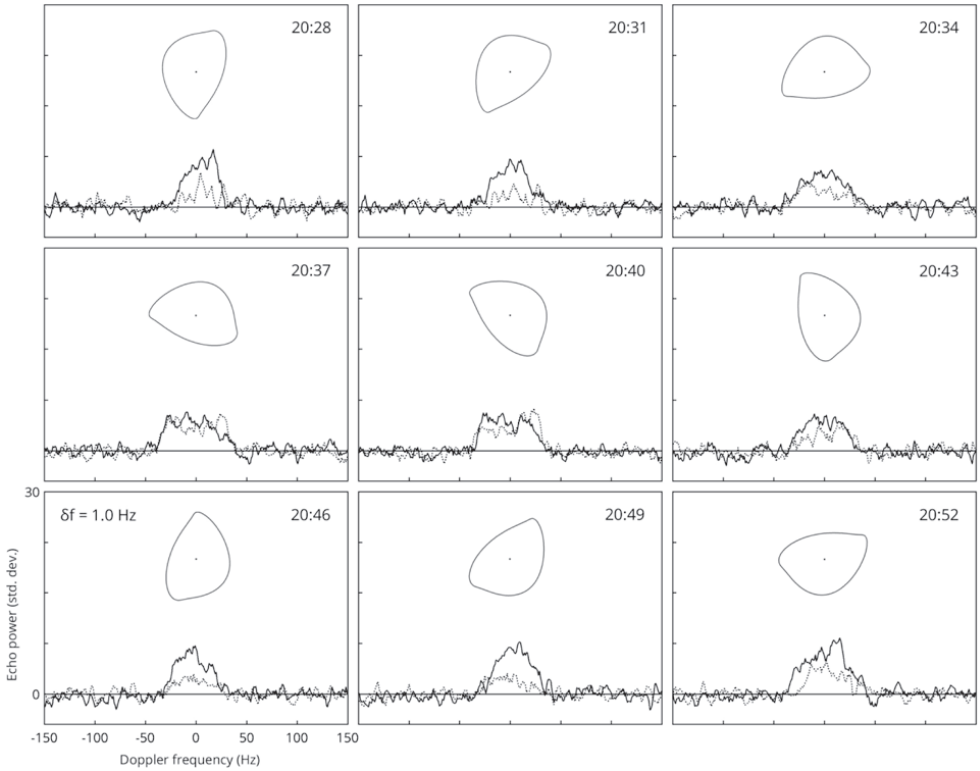

Fig. 6. 2011 UW158 echo spectra and hull at 9 rotation phases obtained at the Zelenchukskaya observatory

Table 1
Heliocentric orbital elements of 2011 UW158 at Epoch 27 June 2015 (TDB)

Quantity	Value	$1-\sigma$ Uncertainty
Mean anomaly (○)	349.644211875983300	2.3×10^{-7}
Argument of perihelion (○)	8.647209242351241	6.0×10^{-7}
Longitude of ascending node (○)	286.272925199741600	3.5×10^{-7}
Inclination (○)	4.649839784639325	1.3×10^{-7}
Eccentricity	0.3751308317245291	7.9×10^{-10}
Mean motion (○/day)	0.4792646070227142	7.6×10^{-10}

6 Summary

The radar echo of the signal transmitted from the 70 m antenna of the Goldstone Observatory was successfully detected. The obtained results confirm the possibility and effectiveness of the bistatic radar observations of near-Earth Asteroids using the 32 m radio telescopes of the “Quasar” VLBI network as a receiving part of a bistatic configuration. It is shown that re-

Table 2

Doppler estimates of echo

UTC epoch 2015-08-18	Zelenchukskaya		Badary	
	Doppler frequency, Hz	$O-C$, Hz	Doppler frequency, Hz	$O-C$, Hz
20:28	54903	−11	58479	−8
20:31	54727	−6	58367	−3
20:34	54550	−3	58246	−7
20:37	54373	1	58135	1
20:40	54190	−2	58016	1
20:43	54011	0	57905	9
20:46	53832	2	57783	7
20:49	53643	−6	57654	0
20:52	53463	−6	57525	−7

ceiving and processing of the continuous wave echo allows us to estimate the value of the Doppler frequency with a sufficient accuracy which can be used to obtain the spin period and size of Near-Earth Objects as well as improve the accuracy in predicting ephemerides. Following this positive experience we have made plans to continue the bistatic radar experiments for obtaining continuous wave spectra and range-Doppler images in the near future.

This work was supported by the Russian Scientific Foundation grant No 16- 12-00071.

References

1. *Benner L. A. M., S. J. Ostro, C. Magri, M. C. Nolan, E. S. Howell, J. D. Giorgini, J. L. Margot, M. W. Busch, M. K. Shepard, P. A. Taylor, R. F. Jurgens* Near-Earth asteroid surface roughness depends on compositional class. — 2008. — Icarus 198. — P. 294–304.
2. *Bondarenko Yu., Vavilov D., Medvedev Yu.* Method of determining the orbits of the small bodies in the solar system based on an exhaustive search of orbital planes. Solar System Research. — 2014. — Vol. 48, Is. 3. — P. 212–216.
3. *Gary, Bruce L.* Unusual Properties for the NEA (436724) 2011 UW158. The Minor Planet Bulletin (ISSN 1052-8091). Bulletin of the Minor Planets Section of the Association of Lunar and Planetary Observers. — 2016. — Vol. 43, No. 1. — P. 33–38.
4. *Grenkov S. A., Nosov E. V., Fedotov L. V., Koltsov N. E.* A Digital Radio Interferometric Data Acquisition System Instruments and Experimental Techniques. — 2010. — Vol. 53, Is. 5. — P. 675–681.

5. *Ipatov A.. Gayazov I., Smolentsev S., Ivanov D., Ilin G., Shuygina N., Bondarenko Yu.* Co-location of Space Geodetic Techniques at the "Quasar" VLBI Network Observatories. VGOS: The New VLBI Network. Proceedings of the 8th IVS General Meeting. Science Press, Beijing, China, 2014. — P. 173–177.
6. *Naidu, Shantanu P., Benner, Lance A M., Brozovic, Marina et al.* Radar observations of near-Earth asteroid (436724) 2011 UW158 using the Arecibo, Goldstone, and Green Bank Telescopes. DPS meeting 47, Book of Abstracts, 2015.
7. *Ostro S. J., Rosema K. D., Jurgens R. F.* The Shape of Eros. — 1990. — Icarus 84. — P. 334–351.
8. *Zaitsev A. L., Ostro S. J., Ignatov S. P., Yeomans D. K., Petrenko A. G., Choate D., Margorin O. K., Cormier R. A., Mardyshkin V. V., Winkler R., Rghiga O. N., Jurgens R. F., Shubin V. A., Giorgini J. D., Krivtsov A. P., Rosema K. D., Koluka Y. F., Slade M. A., Gavrik A. L., Andreev V. B., Ivanov D. V., Peshin P. S., Koyama Y., Yoshikava M., Nakamura A.* Intercontinental bistatic radar observations of 6489 Golevka (1991 JX). Planetary and Space Science. — 1997. — 45. — P. 771–778.